



HAL
open science

Probing the dynamic properties of two sites simultaneously in a protein–protein interaction process: a SDSL-EPR study

N. Le Breton, S. Longhi, A. Rockenbauer, B. Guigliarelli, S. Marque, V. Belle,
M. Martinho

► To cite this version:

N. Le Breton, S. Longhi, A. Rockenbauer, B. Guigliarelli, S. Marque, et al.. Probing the dynamic properties of two sites simultaneously in a protein–protein interaction process: a SDSL-EPR study. *Physical Chemistry Chemical Physics*, 2019, 21 (40), pp.22584-22588. 10.1039/c9cp04660g . hal-03017843

HAL Id: hal-03017843

<https://hal.science/hal-03017843v1>

Submitted on 23 Nov 2020

HAL is a multi-disciplinary open access archive for the deposit and dissemination of scientific research documents, whether they are published or not. The documents may come from teaching and research institutions in France or abroad, or from public or private research centers.

L'archive ouverte pluridisciplinaire **HAL**, est destinée au dépôt et à la diffusion de documents scientifiques de niveau recherche, publiés ou non, émanant des établissements d'enseignement et de recherche français ou étrangers, des laboratoires publics ou privés.

Probing the dynamic properties of two sites simultaneously in a protein-protein interaction process: a SDSL-EPR study

Received 22nd August 2019,
Accepted 26th September 2019

N. Le Breton,^{a,b} S. Longhi,^c A. Rockenbauer,^d B. Guigliarelli,^a S. R. A. Marque,^e V. Belle^{*a} and M. Martinho^{*a}

DOI: 10.1039/c9cp04660g

www.rsc.org/

During molecular processes, protein flexibility is a fundamental property allowing protein-protein interaction. Following structural changes during these interactions is then of crucial interest. Site-Directed Spin Labeling (SDSL) combined to EPR spectroscopy is a powerful technique to follow structural modifications within proteins and during protein-protein interactions. Usual nitroxide labels target cysteine residues and affords a 3-line spectrum, whose shape is informative of the structural environment of the label. However, it is not possible to probe two regions of a protein or two partner proteins at the same time because of overlapping of EPR signatures. Previously, we reported the design and the characterization of a spin label based on a β -phosphorylated (PP) nitroxide yielding a 6-line spectrum. Here, we report the use of two labels with different EPR signatures, namely maleimido-proxyl (P) and PP, to follow structural changes during a protein-protein interaction process in one single experiment. As a model system, we chose a disordered protein that undergoes an induced α -helical folding upon binding to its partner. We show that the EPR spectrum of a mixture of labeled interacting proteins can be analyzed in terms of structural changes during the interaction. This study represents an important step forward in the extension of the panoply of SDSL-EPR approaches.

Introduction

Describing molecular recognition and interaction between proteins is central to understand molecular processes governing life. The current view of these processes is that individual proteins, instead of adopting a single rigid structure, are dynamic entities in constant motion, experiencing structural modifications and having conformational heterogeneity.¹ This fundamental property allows them to function through molecular interactions with other molecules (either substrates, cofactors or proteins) in a wide range of biological processes, such as enzymatic activity regulation, signaling mechanisms, and molecular assembly.² Protein-protein interactions are events that often requires structural flexibility in each partner to enable the association. Allostery is for instance a regulation process that involves protein flexibility in which ligand binding at one site influences binding at another site through a propagated structural change within the protein.³⁻⁴ An extreme example of flexibility is provided by Intrinsically Disordered Proteins (IDPs), *i.e.* functional proteins

devoid of a stable structure under physiological conditions of pH and salinity and in the absence of a partner or ligand.⁵⁻⁸ Two mechanisms have been proposed to explain the folding coupled to binding of Intrinsically disordered proteins (IDPs), *i.e.* conformational selection and induced-fit mechanisms.⁹⁻¹⁰ Site-Directed Spin Labeling (SDSL) combined with Electron Paramagnetic Resonance (EPR) spectroscopy is one of the most powerful techniques to obtain information on protein dynamics.¹¹⁻¹⁴ It is widely used to study structural changes within proteins or reveal interacting regions in protein-protein interactions.¹⁵⁻¹⁶ In particular, SDSL-EPR has been shown to be sensitive enough to enable mapping induced folding events within IDPs.¹⁷⁻²¹ The technique is based on the specific introduction of a paramagnetic label, usually a nitroxide radical, at a chosen cysteine residue (usually introduced by mutagenesis) and its spectral analysis by EPR. Variations of the EPR spectral shapes reflect changes in the dynamics of the spin label environment revealing structural modifications within the protein. Available commercial nitroxide labels, such as 1-oxyl-2,2,5,5-tetramethyl- δ 3-pyrroline-3-methyl (MTSL) or 3-maleimido-2,2,5,5-tetramethyl-1-pyrrolidinyloxy (referred to as P, scheme 1), exhibit typical 3-line spectra, resulting from the hyperfine interaction between the electron spin and the nuclear spin of the ¹⁴N atom (scheme 1). The poor diversity of these EPR signatures precludes simultaneous study of a protein and its partner during interaction or of two different regions of a same protein. To overcome this limitation, we recently proposed a newly synthesized β -phosphorylated nitroxide (referred to as PP, scheme 1) having a phosphorus

^a Aix Marseille Univ, CNRS, BIP, Marseille, France. mmartinho@imm.cnrs.fr and belle@imm.cnrs.fr; Fax: +33-4-9116-4097; Tel: +33-4-9116-4414

^b Université de Strasbourg, CNRS, POMAM, Strasbourg, France (present address)

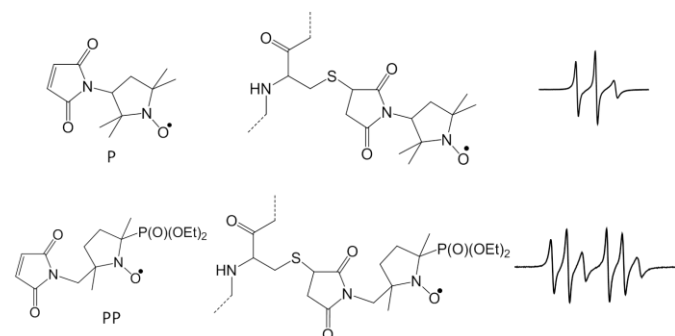
^c Aix Marseille Univ, CNRS, AFMB, Marseille, France.

^d Research Center of Natural Sciences, Budapest University of Technology and Economics, Budapest, Hungary

^e Aix Marseille Univ, CNRS, ICR, Marseille, France.

Electronic Supplementary Information (ESI) available: [EPR spectral shape simulations]. See DOI: 10.1039/c9cp04660g

atom in the vicinity of the NO group.²² The resulting EPR spectrum is a 6-line spectrum (doublet of triplet) arising from a supplementary strong hyperfine coupling between the electron spin and the nuclear spin of the ³¹P atom ($I = \frac{1}{2}$) (typical averaged values are $\bar{A}_P = 5.0$ mT and $\bar{A}_N = 1.4$ mT). In that previous study, we demonstrated that PP is as efficient as P in probing different structural environments and in revealing folding events induced by protein–protein interactions.²²



Scheme 1 Chemical structures of nitroxide radicals: 3-maleimido-2,2,5,5-tetramethyl-1-pyrrolidinyloxy (P) and {2-[(diethoxyphosphoryl)-5-[(2,5-dioxo-2,5-dihydro-1H-pyrrol-1-yl)methyl]-2,5-dimethylpyrrolidin-1-yl] oxidanyl (PP) and their link to cysteine residues with an illustration of the typical 3- or 6-line EPR signatures.

To go further, the present paper aims at demonstrating that the two P and PP labels can be used together to reveal the structural properties and potential structural modifications of two sites in a single experiment during a protein–protein interaction event. As a model of protein–protein interaction, we used the well-described association of the intrinsically disordered C_{term} region of the Measles virus (MeV) nucleoprotein (N_{TAIL} , aa 401–525), and the X domain of the viral phosphoprotein (P_{XD} , aa 459–507).^{23–25} This biological system has been extensively studied using many different approaches,^{26–30} including SDSL-EPR. The latter, allowed mapping the α -helical induced folding of N_{TAIL} upon interaction with P_{XD} to residues 488–502, while the other regions of N_{TAIL} remain highly disordered.^{17, 31}

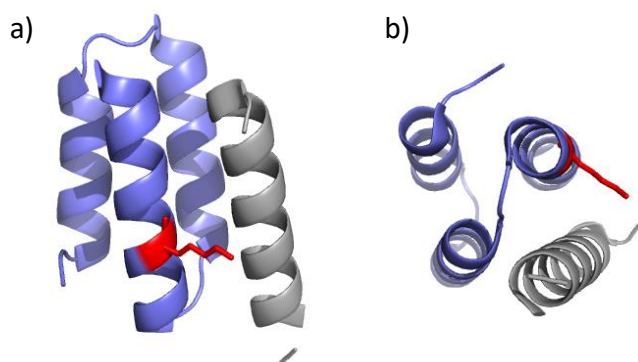


Fig. 1 Crystal structure of the MeV chimera between P_{XD} (residues 459–507) and the N_{TAIL} region encompassing residues 486–504 (pdb code 1T60³²). Lysine 496 of P_{XD} is highlighted in red. (a) lateral view and (b) bottom view.

Here, one position on each partner has been chosen for grafting the paramagnetic label. Within N_{TAIL} , position 407 has been selected as it is known not to be involved in the interaction with P_{XD} .¹⁷ Within P_{XD} , position 496 has been chosen on the basis of the structure of a chimeric construct between P_{XD} and the N_{TAIL} region encompassing residues 486–504 (pdb code 1T60) (Fig. 1).³² In this structure, residue K496 is pointing toward the α -helical N_{TAIL} segment and the label at this position (after Lys to Cys mutation) is expected to be sensitive to the association of the two partners. The objective of this study is to label each partner alternatively with P and PP spin labels and to determine whether structural information can be deduced from the simulation of the complex spectrum resulting from the mixture of the two labeled interacting proteins.

Results and discussion

EPR spectra analyses of the individual labeled proteins

The N_{TAIL} S407C and P_{XD} K496C variants have been constructed, expressed and purified to homogeneity. Each variant has been subsequently labeled with either the P or the PP label. The room temperature (RT) EPR spectra of N_{TAIL} S407C^{P/PP} and P_{XD} K496C^{P/PP} are shown in Figure 2. EPR spectra of N_{TAIL} S407C^{P/PP} are indicative of a high radical mobility (narrow lines) consistent with the disordered character of the protein.¹⁷ EPR spectra of P_{XD} K496C^{P/PP} are still in the rapid regime of mobility of the spin label but show broader lines, in agreement with a label grafted on a structured region and being solvent-exposed.³³ It has to be noted that these EPR spectra reflect the global mobility of the spin label that contains also a contribution coming from the rotational movement of the protein itself, with this being especially the case for P_{XD} that is a small protein (~6 kDa).

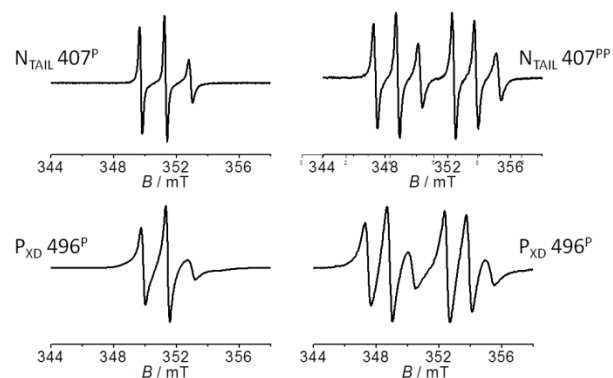


Fig. 2 Amplitude normalized RT EPR spectra of N_{TAIL} S407C^{P/PP} (upper line) and P_{XD} K496C^{P/PP} (lower line). Main recording parameters: microwave power 10mW, magnetic field modulation amplitude 0.1mT.

To go further in the analysis, the EPR spectra were simulated using an extended version of the ROKI software (see experimental section).³⁴ The EPR spectra of N_{TAIL} S407C^{P/PP} can be simulated by one component with a rotational correlation time τ_C of 0.8 (1) ns and 1.3 (2) ns for N_{TAIL} S407C^P and S407C^{PP} respectively (See Table 1). **Details concerning the simulations**

are given in SI (Fig S1 and S2). The EPR spectra of P_{XD} K496C^{P/PP} can be simulated using two components: a narrow one referred to as the component 1 ($\tau_c = 2.6$ (4) ns and 2.8 (4) ns for K496C^P and K496C^{PP} respectively) and a broad one ($\tau_c = 27$ (6) ns for K496C^P and $\tau_c = 30$ (6) for K496C^{PP}) referred to as the component 2 (Table 1). The simulated spectra with the decomposition of the two components are given in SI in Fig. S3. The existence of two components can be attributed to two rotameric states of the spin label, each experiencing a unique environment as already reported in the literature.³⁵⁻³⁶

Table 1. Rotational correlation time τ_c extracted from the simulation of the RT EPR spectra of N_{TAIL} S407C^{P/PP} or P_{XD} K496C^{P/PP} using the ROKI software.³⁴ The relative proportions of each spectral component are given (%).

	N_{TAIL} S407C ^P	N_{TAIL} S407C ^{PP}	P_{XD} K496C ^P	P_{XD} K496C ^{PP}
τ_c (ns)	0.8(1)	1.3(2)	2.6(4) 27(6)	2.8(4) 30(6)
%	100	100	45(5) 55(5)	45(5) 55(5)

EPR spectra analysis of mixtures of the labeled proteins

The labeled species were mixed in a 1:1 ratio to ensure that none of the EPR signal dominates the other. Fig. 3 shows the EPR spectra resulting from the mixture of the different possible combinations. Mixing N_{TAIL}^P with P_{XD}^P led to a 3-line spectrum (mixture 1, Fig. 3a) in which it is impossible to distinguish the individual signature of each labeled protein. Even if the simulation can be obtained, it is not possible to attribute without ambiguity one component to one site, especially if there are spectral shape modifications resulting from the interacting proteins. This resulting spectrum shows the limitation of the use of classical spin labels for probing two sites simultaneously. In this case, no information can be derived from the mixture of these two labeled species. On the contrary, interaction between N_{TAIL}^{PP} and P_{XD}^P (mixture 2, Fig. 3b) or N_{TAIL}^P and P_{XD}^{PP} (mixture 3, Fig. 3c) gives rise to a complex EPR spectrum in which the two EPR signatures arising from P and PP are partially overlapping but still distinguishable (Fig. S4). The fact that the individual signatures can be distinguished enables the simulation of the whole spectrum.

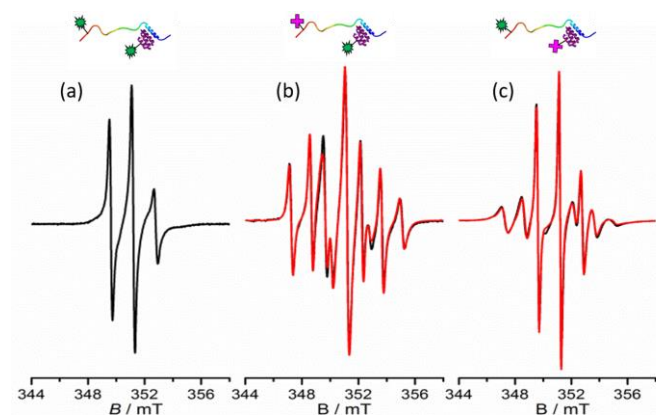


Fig 3. RT EPR spectra of equimolar mixtures of (a) mixture 1: N_{TAIL} S407C^P and P_{XD} K496C^P, (b) mixture 2: N_{TAIL} S407C^{PP} and P_{XD} K496C^P, (c) mixture 3: N_{TAIL} S407C^P and P_{XD} K496C^{PP}. The spectra shown in panels (b) and (c) have been simulated using the ROKI

software³⁴ (red). An illustration of the complex $N_{TAIL}(\text{rainbow}):P_{XD}(\text{purple})$ is given with the indication of the labels P (green star) and PP (pink cross).

Table 2 summarizes the results of the simulation of each composite spectrum. The decomposition of each simulated spectra are given in SI in Fig. S5. For the position 407 of N_{TAIL} (P and PP) the same parameters as those determined in the absence of P_{XD} were found (Table 1). This result confirms that this N_{TAIL} region is unaffected by $N_{TAIL}:P_{XD}$ complex formation and that it fully retains its disordered character. On the contrary, concerning P_{XD} , the values of τ_c are different from the ones found with P_{XD} alone. The two components attributed to different rotameric states of the labels are still present but the values of τ_c increase (from 2.6-2.8 to 5.1-5.2 ns for component 1 and from 27-30 to 50 ns for component 2). Note that the proportion of component 1 with respect to component 2 is significantly different in the case of P_{XD} K496C^{PP} bound to N_{TAIL} (25%/75%) compared to P_{XD} K496C^{PP} alone (Table 1) or to P_{XD} K496C^P in complex (Table 2). This difference is probably due to the reorientation of the PP label in the complex. For both composite spectra, the increased values of τ_c for the labels at position 496 of P_{XD} reveal that this site is part of the interaction site between N_{TAIL} and P_{XD} as expected from the structure of the chimera construct (Fig. 1).³² Note that the reliability of this structural model, obtained using an artificial chimeric construct, has already been validated by our previous SDSL-EPR results.¹⁷

Table 2. Rotational correlation time τ_c extracted from the simulation of the RT EPR spectra of N_{TAIL} S407C^{P/PP} in the presence of P_{XD} K496C^{P/PP}, using the ROKI software.³⁴ The relative proportions of each spectral component are given (%).

	Mixture 2			Mixture 3		
	N_{TAIL} S407C ^{PP}	P_{XD} K496C ^P	P_{XD} K496C ^{PP}	N_{TAIL} S407C ^P	P_{XD} K496C ^P	P_{XD} K496C ^{PP}
τ_c (ns)	0.8(1)	5.1(4) 50(8)	5.2(4) 50(8)	1.3(2)	5.2(4) 50(8)	5.2(4) 50(8)
%	100	60(5) 40(5)	75(5) 25(5)	100	75(5) 25(5)	75(5) 25(5)

Simulation of EPR spectra of the mixture of N_{TAIL} S407C^{P/PP} and P_{XD} K496C^{P/PP} can then be achieved, giving simultaneous structural information during protein-protein interaction. Thus, the combined use of these two different nitroxide labels with different EPR signatures gives the opportunity to follow structural changes on two proteins at the same time. It should be mentioned that, as PP has a broader spectral width compared to P, the detection of PP grafted to a protein requires higher protein concentrations. Another limitation can arise from the high complexity of the resulting spectrum (6+3 lines) that may, in some cases, be too difficult to simulate if the 3-lines overlap too much the 6-lines.

Experimental

Chemicals

Unless otherwise noted, all chemicals and solvents were of analytical grade and used without further purification.

Synthesis of PP

The synthesis and full characterization of PP has been already described.²²

Protein expression and purification

The cysteine-substituted N_{TAIL} variant was prepared as previously described.^{17, 31} Expression and purification of the cysteine-substituted P_{XD} variant was prepared as already described,²⁶ except that a washing step with 2 M NaCl was added prior to elution from the immobilized metal affinity chromatography (IMAC) column and that a nickel resin was used instead of cobalt resin.³⁰ Protein concentrations were calculated using OD₂₈₀ measurements and the theoretical absorption coefficients ϵ (mg/mL.cm) at 280 nm, as obtained using the program ProtParam from the ExpASY server.

Labeling procedures

Before spin labeling, dithiothreitol (DTT) was added to the purified variant (N_{TAIL} S407C and P_{XD} K496C) (approximately 1.5 mg) in a molar excess of 100. The mixture was incubated for 30 min in an ice bath to reduce the unique free cysteine residue. DTT was removed by a PD10 desalting column (GE Healthcare) using 10 mM MES, 150 mM NaCl pH 6.5 as elution buffer. The fractions containing the protein were pooled. Spin labels were immediately added to the sample at a molar excess of 10 using a spin label (P or PP) stock solution at 40 mM in acetonitrile. The reaction was carried out for 1 h in the dark in an ice bath, under gentle stirring and a continuous flow of argon to avoid oxidation. The excess of unbound spin label was removed by gel filtration as described above, except that 10 mM sodium phosphate pH 7.0 was used as elution buffer. The fractions giving an EPR signal, reflecting effective protein labeling, were pooled and concentrated by ultrafiltration using a 5 kDa cutoff polyethersulfone membrane (Vivaspin, Sartorius) in the case of the N_{TAIL} variant, and a 3kDa cutoff Millipore Ultracell low-binding regenerated cellulose membrane (Amicon, Millipore) for the P_{XD} variant. In the case of the P_{XD} K496C variant, the best yield (for both P and PP) was obtained when labeling was conducted in a glove box. Labeling yields were calculated by dividing the spin concentration over the protein concentration. Labeling yields obtained for N_{TAIL} S407C^P was around 100% whereas for N_{TAIL} S407C^{PP} only 50% was achieved. For P_{XD} K496C^{P/PP} labeling yields ranged from 90 to 100 %.

EPR spectroscopy

EPR spectra were recorded at room temperature on an ELEXSYS E500II Bruker spectrometer equipped with an ELEXSYS Super High Q sensitivity resonator operating at 9.9 GHz. The microwave power was 10 mW, the magnetic field modulation frequency and amplitude were 100 kHz and 0.1 mT, respectively. The concentration of labeled proteins was evaluated by double integration of the EPR signal recorded under non-saturating conditions and comparison with that given by a MTSL standard sample. Protein concentrations were either calculated using OD₂₈₀ measurements and the theoretical absorption coefficients ϵ (mg/mL.cm) at 280 nm, as obtained using the program ProtParam at the ExpASY server,

or measured using the Biorad protein assay (Bio-Rad Laboratories, Hercules, CA). The labeling yields were estimated by calculating the ratio between the concentration of labeled proteins and the total protein concentration. Labeling yields ranged from 50 to 100 %. Protein concentrations of 50 μ M were used to record individual EPR spectra. All spectra were recorded at RT, from protein samples in 10 mM sodium phosphate at pH 7.0.

EPR spectral shape simulations

EPR spectra of individual variants labeled with PP or P were simulated using an extended version of the ROKI software.³⁴ For the simulation of the spectra of mixtures of N_{TAIL} S407C and P_{XD} K496C labeled with P or PP, 3 components (one narrow for N_{TAIL} S407C^{P/PP} and one broad and one narrow for P_{XD} K496C^{P/PP}) were added so as to obtain the best fit to experimental data.

Conclusions

The aim of this study is to simultaneously (*i.e.* in one single experiment) follow and analyze structural changes within two proteins involved in a protein-protein interaction. Conventional SDSL-EPR approaches are limited due to the poor diversity of the EPR signatures of nitroxide radicals (3-line spectra). To overcome this limitation, we proposed to combine the use of two different spin labels having two distinct EPR signatures: a conventional nitroxide (maleimido proxyl P) and a phosphorylated one (PP). By choosing a well-described of protein-protein interaction model system, we show that the composite spectrum resulting from the mixture of the two labeled interacting partners can be analyzed only if P is grafted on one site and PP on the other. On the contrary, if P is the label for the two sites, the mixture leads to a spectrum that cannot be analysed due to a too important overlap of the two signals. P and PP are both nitroxide spin labels designed to target cysteine residues, which precludes their combined use to explore two sites of a same protein simultaneously. Our recent development of nitroxide targeting tyrosine residues opens the perspective to overcome this limitation.³⁷⁻³⁹ The combination of these approaches (targeting different residues, *i.e.* cysteine and tyrosine, and using two different nitroxide labels to target these residues) opens up new perspectives to follow structural changes within proteins. Additionally, the method can be extended to the study of other types of interactions between biomolecules such as protein-RNA or RNA-RNA interactions, with the latter case though requiring the synthesis of appropriate phosphorylated nitroxides. To conclude, this study constitutes a new step in the enlargement of the panoply of SDSL-EPR approaches.

Acknowledgements

This work was supported by the Agence Nationale de la Recherche ANR SPINFOLD n° 09-BLAN-0100, the Centre National de la Recherche Scientifique (CNRS) and Aix-Marseille

Université. The authors are also grateful to the EPR facilities available at the national EPR network (IR CNRS 3443) and the Aix-Marseille Université EPR center. The authors also wish to acknowledge David Blocquel (AFMB lab) for technical help during the purification of the N_{TAIL} S407C and P_{XD} K496C variants. NLB is grateful to Aix Marseille Université and PACA region for her PhD fellowship. We acknowledge the support of the Hungarian National Research, Development and Innovation Office (NKFIH) Grant (K119442).

Conflicts of interest

There are no conflicts to declare.

References

1. K. Henzler-Wildman; D. Kern, *Nature*, 2007, **450** (7172), 964-972.
2. K. Teilum; J. G. Olsen; B. B. Kragelund, *Cell. Mol. Life Sci.*, 2009, **66** (14), 2231-2247.
3. K. Gunasekaran; B. Y. Ma; R. Nussinov, *Proteins: Struct. Funct. Bioinf.*, 2004, **57** (3), 433-443.
4. N. M. Goodey; S. J. Benkovic, *Nature Chemical Biology*, 2008, **4** (8), 474-482.
5. T. Chouard, *Nature*, 2011, **471** (7337), 151-153.
6. M. M. Babu; R. van der Lee; N. S. de Groot; J. Gsponer, *Curr. Opin. Struct. Biol.*, 2011, **21** (3), 432-440.
7. V. N. Uversky; A. K. Dunker, *BBA-Proteins Proteom.*, 2010, **1804** (6), 1231-1264.
8. P. Tompa, *Trends Biochem. Sci.*, 2002, **27** (10), 527-33.
9. J. Habchi; P. Tompa; S. Longhi; V. N. Uversky, *Chem. Rev.*, 2014, **114** (13), 6561-6588.
10. P. Csermely; R. Palotai; R. Nussinov, *Trends in Biochemical Sciences*, 2010, **35** (10), 539-546.
11. E. Bordignon; S. Bleicken, *BBA-rev Biomembranes*, 2018, **1860** (4), 841-853.
12. W. L. Hubbell; C. J. Lopez; C. Altenbach; Z. Y. Yang, *Curr. Opin. Struct. Biol.*, 2013, **23** (5), 725-733.
13. J. P. Klare; H. J. Steinhoff, In *Structural Information from Spin-Labels and Intrinsic Paramagnetic Centres in the Biosciences*, Timmel, C. R.; Harmer, J. R., Eds. 2014; Vol. 152, pp 205-248.
14. M. Martinho, Fournier, E., Le Breton, N., Mileo, E. and Belle V., In *Electron Paramagnetic Resonance*, Chechik, V., Murphy, D., Ed. Royal Society of Chemistry: 2019; Vol. 26, pp 66-88.
15. M. Lorenzi; L. Sylvi; G. Gerbaud; E. Mileo; F. Halgand; A. Walburger; H. Vezin; V. Belle; B. Guigliarelli; A. Magalon, *PLoS one*, 2012, **7** (11), 10.1371/journal.pone.0049523.
16. V. Belle; A. Fournel; M. Woudstra; S. Ranaldi; F. Prieri; V. Thomé; J. Currault; R. Verger; B. Guigliarelli; F. Carrière, *Biochemistry*, 2007, **46** (8), 2205-2214.
17. V. Belle; S. Rouger; S. Costanzo; E. Liquière; J. Strancar; B. Guigliarelli; A. Fournel; S. Longhi, *Proteins: Struct. Funct. Bioinf.*, 2008, **73** (4), 973-988.
18. N. L. Pirman; E. Milshteyn; L. Galiano; J. C. Hewlett; G. E. Fanucci, *Protein Sci.*, 2011, **20** (1), 150-159.
19. M. Martinho; J. Habchi; Z. El Habre; L. Nesme; B. Guigliarelli; V. Belle; S. Longhi, *J. Biomol. Struct. Dyn.*, 2013, **31** (5), 453-471.
20. T. M. Casey; Z. L. Liu; J. M. Esquiaqui; N. L. Pirman; E. Milshteyn; G. E. Fanucci, *Biochem. Biophys. Res. Comm.*, 2014, **450** (1), 723-728.
21. M. Palombo; A. Bonucci; E. Etienne; S. Ciurli; V. N. Uversky; B. Guigliarelli; V. Belle; E. Mileo; B. Zambelli, *Sci. Rep.*, 2017, **7** (1), 5977.
22. N. Le Breton; M. Martinho; K. Kabytaev; J. Topin; E. Mileo; D. Blocquel; J. Habchi; S. Longhi; A. Rockenbauer; J. Golebiowski; B. Guigliarelli; S. R. A. Marque; V. Belle, *Phys. Chem. Chem. Phys.*, 2014, **16** (9), 4202-4209.
23. J. M. Bourhis; V. Receveur-Bréchet; M. Oglesbee; X. Zhang; M. Buccellato; H. Darbon; B. Canard; S. Finet; S. Longhi, *Protein Sci.*, 2005, **14**, 1975-1992.
24. D. Karlin; S. Longhi; B. Canard, *Virology*, 2002, **302** (2), 420-32.
25. S. Longhi; V. Receveur-Brechot; D. Karlin; K. Johansson; H. Darbon; D. Bhella; R. Yeo; S. Finet; B. Canard, *J. Biol. Chem.*, 2003, **278** (20), 18638-48.
26. J. Bourhis; K. Johansson; V. Receveur-Bréchet; C. J. Oldfield; A. K. Dunker; B. Canard; S. Longhi, *Virus Research*, 2004, **99**, 157-67.
27. J. Habchi; S. Blangy; L. Mamelli; M. R. Jensen; M. Blackledge; H. Darbon; M. Oglesbee; Y. L. Shu; S. Longhi, *J. Biol. Chem.*, 2011, **286** (15), 13583-13602.
28. J. Habchi; S. Longhi, *Mol. Biosys.*, 2012, **8** (1), 69-81.
29. C. G. Bischak; S. Longhi; D. M. Snead; S. Costanzo; E. Terrer; C. H. Londergan, *Biophysical Journal*, 2010, **99** (5), 1676-1683.
30. D. Blocquel; J. Habchi; S. Costanzo; A. Doizy; M. Oglesbee; S. Longhi, *Protein Science*, 2012, **21** (10), 1577-1585.
31. B. Morin; J. M. Bourhis; V. Belle; M. Woudstra; F. Carrière; B. Guigliarelli; A. Fournel; S. Longhi, *J. Phys. Chem. B*, 2006, **110** (41), 20596-20608.
32. R. L. Kingston; D. J. Hamel; L. S. Gay; F. W. Dahlquist; B. W. Matthews, *Proc. Natl. Acad. Sci. USA*, 2004, **101** (22), 8301-6.
33. H. S. Mchaourab; M. A. Lietzow; K. Hideg; W. L. Hubbell, *Biochemistry*, 1996, **35** (24), 7692-704.
34. A. Rockenbauer; L. Korecz, *Appl. Magn. Reson.*, 1996, **10** (1-3), 29-43.
35. Z. F. Guo; D. Cascio; K. Hideg; W. L. Hubbell, *Protein Sci.*, 2008, **17** (2), 228-239.
36. Z. F. Guo; D. Cascio; K. Hideg; T. Kalai; W. L. Hubbell, *Protein Sci.*, 2007, **16** (6), 1069-1086.
37. M. Lorenzi; C. Puppo; R. Lebrun; S. Lignon; V. Roubaud; M. Martinho; E. Mileo; P. Tordo; S. R. A. Marque; B. Gontero; B. Guigliarelli; V. Belle, *Angew. Chem. Int. Edit.*, 2011, **50** (39), 9108-9111.
38. E. Mileo; E. Etienne; M. Martinho; R. Lebrun; V. Roubaud; P. Tordo; B. Gontero; B. Guigliarelli; S. R. A. Marque; V. Belle, *Bioconj. Chem.*, 2013, **24** (6), 1110-1117.
39. C. Gmeiner; D. Klose; E. Mileo; V. Belle; S. R. A. Marque; G. Dorn; F. H. T. Allain; B. Guigliarelli; G. Jeschke; M. Yulikov, *J. Phys. Chem. Lett.*, 2017, **8** (19), 4852-4857.